

1 **ECO-FRIENDLY PANELS MADE OF AUTOCLAVED FLAX COMPOSITES AND**
2 **UPCYCLED BOTTLE CAPS CORE: EXPERIMENTAL AND NUMERICAL APPROACH**

3 **Pablo R. Oliveira^{a,b}, Michael May^a, Sebastian Kilchert^a, Livia A. Oliveira^{c,d}, Túlio H. Panzera^{c,d},**
4 **Vincent Placet^e, Fabrizio Scarpa^f, Stefan Hiermaier^{a,b}**

5
6 ^a Fraunhofer EMI, Ernst-Mach Institut, Freiburg im Breisgau, Germany

7 ^b Department of Sustainable Systems Engineering – INATECH, Albert-Ludwigs-Universität Freiburg,
8 Freiburg im Breisgau, Germany.

9 ^c Centre for Innovation and Technology in Composite Materials – CITeC, Department of Mechanical
10 Engineering - PPMEC, Federal University of São João del Rei-UFSJ, São João del Rei, Brazil

11 ^d Department of Natural Sciences - FQMat, Federal University of São João del Rei-UFSJ, Brazil

12 ^e Department of Applied Mechanics, Université Bourgogne Franche-Comté, FEMTO-ST Institute,
13 CNRS/UFC/ENSMM/UTBM, 25000 Besançon, France

14 ^f Bristol Composites Institute - ACCIS, University of Bristol, BS8 1TR Bristol, UK

15
16 **Abstract:** *The use of recycled and renewable components in structural applications supports the*
17 *development of sustainable lightweight structures. Disposed bottle caps can be used to generate eco-*
18 *friendly honeycomb cores, especially when combined with other eco-friendly components. A natural*
19 *fibre-based laminate represents an alternative to synthetic fibres, matrices, and metals in skins for*
20 *sandwich panels. This study evaluates the use of flax fibre laminates as sustainable skins for sandwich*
21 *panels made from upcycled bottle caps core. Metallic skin cases are also tested as a reference. The*
22 *influence of the amount of adhesive used to produce the panels is also investigated in a 2² full factorial*
23 *design, together with an independent test carried out on samples made from natural fibres. The*
24 *characterisation against flexural and low-velocity dynamic loads indicates that the flax fibre skin leads*
25 *to specific core shear and flexural moduli up to 19% higher than in aluminium-based panels.*
26 *Unidirectional flax fibres, however, reduce the energy absorption during impact. Flexural properties*
27 *show that the most efficient design involves the least adhesive amount. Finite element models also show*
28 *a good fit to the experimental results and indicate a 166% increase of energy absorption with the*
29 *presence of multidirectional fibre laminates.*

30 **Keywords:** bottle caps, flax fibre laminate, FE models, design of experiment, sustainability.

31 **1. INTRODUCTION**

32 The investigation of sustainable structures for the construction and automotive industry is a recent
33 movement following environmental regulations and demand from end-users [1,2]. The design of
34 lightweight applications and the use of components with reduced ecological impact are some initiatives
35 to obtain greener products. Sandwich panels are a suitable solution for the development of a low-cost

1 and effective structure with less environmental damage. The increase in the second area moment with a
2 thick light core between two thin skins increases the bending resistance of sandwich structures without
3 compromising its lightweight design [3]. The use of eco-friendly parts, such as recycled or renewable
4 skins, adhesive and core, contribute to improving the sustainability of the sandwich panel [4,5].

5 Natural fibre laminates are promising components to be used in sandwich panel skins. Reduced
6 cost, less energy demand for extraction, high biodegradability and good mechanical properties are some
7 of their advantages [6]. The scatter of mechanical properties, the limited optimal inclusion in laminates,
8 and the reduced adhesion to polymeric matrices are some drawbacks of natural fibres, which can be
9 minimised by chemical pre-treatments [7,8]. Several renewable fibres have been investigated, such as
10 sisal fibres in fibre-metal laminate (FML) cores [9–11], coconut mesocarp as bio-core [12], piassava
11 skin and sawdust as honeycomb core [13], cotton laminates with bio-PU matrix [14], sugarcane bagasse
12 composites [15,16], and flax fibres as skins and core. Flax fibre (FF) laminates are the first choice when
13 using natural fibres due to their superior mechanical properties [17,18]. The use of FF as a skin combined
14 with natural cores made of cork showed a flexural performance comparable to glass fibre-based (GF)
15 panels [19]. Sandwich structures with FF skins presented better performance in the unidirectional
16 laminate configuration than bidirectional laminate [20]. In addition, the fibrous and cellular structure of
17 the FF contributed to increase the damping ratio and sound absorption capacity of the panels compared
18 to GF, despite the lower impact resistance [21].

19 The sandwich panels are especially dependent on the bonding between parts due to the reduced
20 weight and lower stress concentration of structures bonded with adhesive [22]. The use of recyclable,
21 bio-sourced and upcycled components in the core is an alternative for obtaining sustainable sandwich
22 panels. Adhesives made from plants and beans ensure high adhesion properties with low cost and less
23 environmental impact [23,24]. The inclusion of fillers, such as a recycled rubber particles, can provide
24 an increase in the damping ratio of the structures and in the adhesion properties of a bio-based
25 polyurethane from castor oil [25]. Additionally, natural cores such as bamboo represent some natural-
26 based solutions [26,27]. Thermoplastic-based cores can also facilitate panel recyclability and end-of life
27 disposal and provide good mechanical properties [28,29]. Cabrera et al. [30] designed a recyclable
28 sandwich panel made entirely of polypropylene (PP) with good mechanical properties. One component
29 that has been successfully tested as recycled core is the disposed bottle cap. Bottle caps have a high rate
30 of disposal in landfills and are one of the items most found in cleaning works in seas and oceans [31].
31 The dissimilar composition of plastic bottles and caps reduces the recycling rate of the latter [32]. The
32 enhanced mechanical performance and the tubular geometry of the bottle caps enable their use as a
33 recycled honeycomb core, as previously investigated [5,33–35]. Tubular honeycombs presented a higher
34 yield stress, energy absorption, and fatigue load compared to conventional hexagonal honeycombs [36].
35 The investigation of eco-friendly materials for bottle cap panels has shown adequate mechanical
36 performance with a hybrid configuration with aluminium skin and a bio-based adhesive [5].

1 An appropriate balance between high mechanical performance and reduced environmental impact
 2 is a timely requirement in modern structural applications. The use of natural fibre skins and bottle caps
 3 in sandwich panels has been previously investigated by the authors with promising results [37]. Panels
 4 with coir laminates skins and thinner bottle caps as core exhibited satisfactory specific performance
 5 compared to aluminium skin-based configurations. The thick laminate skin and the high amount of
 6 adhesive found in this panel, however, indicate the need to improve the structure with lightweight
 7 components [37]. This paper progresses those studies by evaluating a laminate made with flax fibres as
 8 an eco-friendly alternative to aluminium skins. The laminates are used in sandwich panel configurations
 9 with bottle caps and are tested under quasi-static and dynamic loads. The effect of the amount of
 10 adhesive on the mechanical properties of the core is investigated in a full factorial design. A finite
 11 element (FE) model is developed for characterisation and optimisation of the laminate setting.

12

13 2. MATERIALS AND METHODS

14 2.1. Materials

15 Unidirectional (UD) flax fibre laminates $[0]_3$ are used as sustainable sandwich panel skins. Pre-
 16 prepreg flaxtape laminates sourced by EchoTechnilin (Lineo, France) are based on flax fibres impregnated
 17 with fire retardant epoxy polymer XB 3515 GB (Huntsman), Aradur 1571 BD, and accelerator 1573
 18 BD. The fibre volume fraction is estimated at $\sim 56\%$ and the lamina thickness is ~ 0.5 mm. Aluminium
 19 skins type AW-5754 with thickness 0.5 mm are used as reference skins. The high-density polyethylene
 20 (HDPE) plastic caps of Brazilian *Coca-Cola*TM bottles, collected after disposal, are used as sustainable
 21 honeycomb core. The bottle caps are cleaned with a degreasing solution and dried at room temperature
 22 for 24 h. The epoxy polymer (resin RenLam-M and hardener GP456, a mixing ratio of 5:1) is used as
 23 an adhesive. The main properties are shown in Table 1.

24

Table 1. Mechanical properties of skin and adhesive components.

Panel component	Young's Modulus (GPa)	Tensile Strength (MPa)
Aluminium AW-5754	70.6 (± 3.5)	246.6 (± 3.2)
Flax laminate (in fibre direction) [38]	35.6 (± 4.7)	300.5 (± 22.5)
Pristine Epoxy [25]	1.9 (± 0.2)	30.8 (± 2.5)
Plastic caps (HDPE polymer) [33]	1.0 (± 0.1)	16.7 (± 1.5)

25

26 2.2. Factorial design

27 A 2^2 full factorial design is conducted following the Design of Experiment (DoE) technique to
 28 assess the effect of the skin type and the amount of adhesive on the mechanical performance of the
 29 panels produced (Table 2). The first factor compares a sustainable natural skin (flax fibre laminate) and
 30 a classic skin (aluminium skin) with the approximate thickness (~ 0.5 mm). The second factor evaluates
 31 the amount of adhesive applied in previous researches (equivalent to a uniform adhesive layer of
 32 thickness 1.5 mm [5,34]) and a reduction in the amount of adhesive by 33.3% (~ 1 mm adhesive layer),

1 as developed in the first bottle caps panel design [33]. An additional condition with 66.7% less adhesive
 2 (~ 0.5 mm adhesive layer) is also conducted for flax fibre panel in an independent test to check a possible
 3 lower limit for weight optimisation of the panel design. The adhesive amount is identified by the nominal
 4 thickness of a uniform adhesive layer. The polymer, however, flows around the plastic caps due to the
 5 dissimilar surface contact between the closed cap surface and the skins, creating a moderate variation in
 6 the adhesive thickness [34]. Three samples are produced per experiment and replicate. The results are
 7 analysed in the Minitab v18 software to verify the significance of the factors studied [39].

8 Table 2. Independent factorial designs for flexural and low-velocity impact tests.

Experiments	Condition	Type of skin	Adhesive amount (nominal thickness)
2² factorial design	C1	Aluminium	1.5 mm
	C2	skin	1.0 mm
	C3	Flax skin	1.5 mm
	C4		1.0 mm
Extra test	C5	Flax skin	0.5 mm

9 **2.3. Manufacturing process**

10 **2.3.1. Flax fibre**

11 Three layers of UD prepreg flax tape are laid up $[0]_3$ and cured in the autoclave at constant
 12 pressure (0.7 MPa) and controlled cyclic temperature (temperature levels of 80°C and 140°C kept
 13 constant for 100 minutes). The laminates are manufactured in their final dimensions to avoid further
 14 damage during cutting: $240 \times 90 \text{ mm}^2$ for flexural tests, and $150 \times 150 \text{ mm}^2$ for impact tests. After
 15 manufacture, the laminates are packed in sealed bags and unpacked only during panel preparation.

17 **2.3.2. Panel**

18 The manufacturing process follows previous work procedures, including control of room
 19 temperature and relative humidity (~22°C and 55% RH) [5, 34]. The aluminium skin is cleaned with a
 20 degreasing solution and sanded in the direction of $\pm 45^\circ$ to increase adhesion to the surface. The surface
 21 of the flax fibre laminate is not treated to prevent damage to the fibres. The skin is introduced into the
 22 mould covered with a release tape (Fig. 1a) and the adhesive is spread over the skin with a wooden stick.
 23 The bottle caps are placed in alternated directions [33] and in a cubic packing [34] on the skin (Fig. 1b)
 24 and the partial sample is left for curing under constant compaction pressure for 24h. After the initial
 25 curing, the second skin is bonded to the core following a similar procedure. The finished samples are
 26 stored in sealed bags for 7 days before being tested (Fig. 1c).

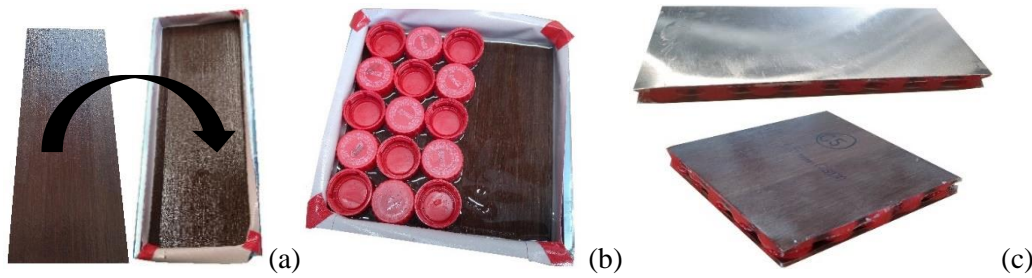


Figure 1. Manufacturing process for sandwich panels: finished skins in the mould (a), bonding of caps core (b) and finished samples of both skins for flexural and impact tests (c).

2.4. Characterisation

2.4.1. Flexural test

The three-point flexural test (3PB - Fig. 2a) is conducted on a Zwick Allroundline machine with a 200 kN load cell, span of 150 mm and displacement rate of 4 mm/min, following the guidelines of ASTM C393 [40], as developed in previous studies for future comparison of the different designs for the bottle caps panels. The sample size is $240 \times 90 \text{ mm}^2$ and thickness 13.5 to 14.2 mm, depending on the adhesive amount. The mechanical responses are the equivalent flexural modulus (E_{flex} - ASTM D790 [41]), the core shear and skin stress (τ_{core} and σ_{skin} - ASTM C393 [40]), and the core shear modulus (G_{core} - ASTM D7250 [42]). Specific properties are calculated as in previous works [5,34] by equivalent panel density (ASTM C20 [43]).

2.4.2. Impact test

A Drop-Tower impact test is performed by following the ASTM D7136 guidelines [44] (Fig. 2b). Samples of 150 mm^2 are simply supported by a square frame with an unsupported area of $125 \times 125 \text{ mm}^2$ and impacted by a semi-spherical impactor of 10 kg under an energy level of $\sim 50 \text{ J}$ ($\pm 3 \text{ J}$). The aluminium tip diameter is 50 mm (bigger than the cell size, as indicated [44]). The test is recorded by a high-speed camera (FASTCAM SA-X type 324K-M2 – 20,000 frames per second) to verify the impactor velocity during the test by digital image correlation. The responses are the maximum load at impact (P_{max}), energy absorption (W_{abs}), the ratio of absorbed energy to the total energy impact (W_{ratio}) and the relevant weight specific-properties (P_{spec} , W_{spec}) [44].

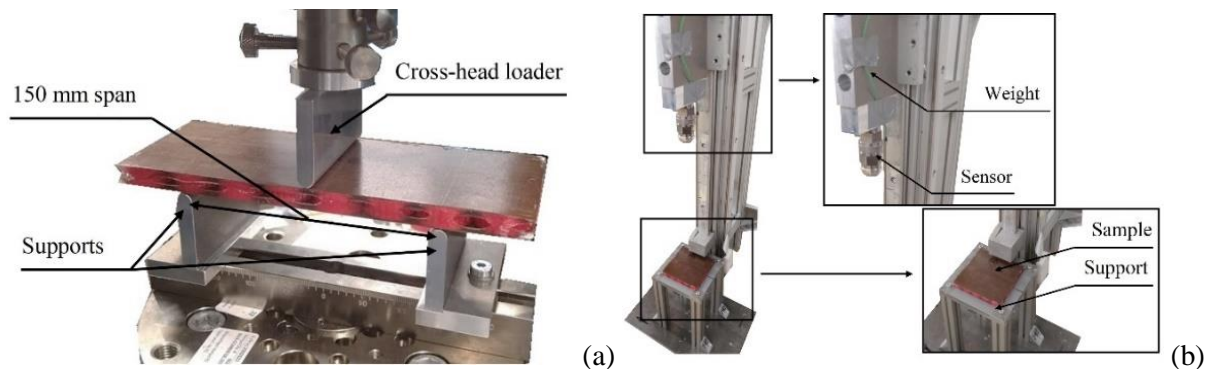


Figure 2. Experimental setup: flexural (a) and drop-tower impact test (b).

1
2
3
4
5
6
7
8
9
10
11
12
13
14
15
16
17
18
19
20
21
22
23
24
25
26
27
28
29
30
31
32
33
34
35
36
37

2.4.3. FE simulations

FE simulations of the proposed designs are developed in *LS-Dyna* software for comparison with experimental results and optimisation of the sandwich panel features. The aluminium skin and the polymeric core (caps + epoxy adhesive) are modelled using an isotropic material model with elastoplastic response and strain hardening defined by the tangent modulus (MAT-024 in *LS-Dyna*). The flax laminates are modelled using the Chang-Chang model available in LS-Dyna as MAT-054/55 in *LS-Dyna*. The model differentiates the fibre and matrix responses, and it is based on the laminate effective failure strain. The models are calibrated using the data provided in Table 1 and Table 9 (section 3.4).

The skin is modelled using Belytschko-Tsay shell elements with three integration points through the skin thickness, while the caps core is based on single integration point constant stress solid elements, which are highly efficient. A composite setting is attributed to the shell laminate configuration, with three unidirectional layers of ~ 0.17 mm thickness each. An automatic surface-to-surface contact is applied between the specimen and the impactor/support to prevent undesired penetrations. The connection between the skin and the bottle caps/adhesive core is based on a tied contact with offset, whose failure is induced by the individual failure of the components, as observed in previous research [35]. The geometric representation (impactor and support dimensions) and the boundary conditions (support type, displacement rate, impact energy) of the testing setup of the finite element model in the *LS-Dyna* are based on the experimental setup. The support and the loader are constrained against displacement and rotation, except in z-direction displacement. The quasi-static loader is based on a constant displacement rate, while an initial velocity is attributed to the ~ 10 kg dynamic impactor of spherical geometry. Mass scaling is used to reduce the simulation time for the quasi-static analyses. The amount of mass scaling is limited to ensure that the effects of inertia do not affect the simulation results.

3. RESULTS

The results of the mechanical tests are summarized in Tables 3 and 4. The specific properties are also calculated according to previous works [5,34]. The experimental curves of both tests are shown in Figure 3, with a preliminary comparison of the factors considered in this work. Flax laminates reduce the overall flexural strength and stiffness of the panel under the 3PB test compared to aluminium panels, decreasing the maximum load and slope of the curve in the elastic region. The ductility of the sample is significantly reduced with flax fibre skins (Fig. 3a) by a sudden drop in the flexural load due to rapid skin debonding. The type of failure for each sample is described in item 3.4. Flax-based samples also experience a significant reduction in the impact load and the duration of the impact event (Fig. 3c). The amount of adhesive also affects the behaviour of the flax-based panel, reducing the maximum flexural and impact load by 47% and 49%, respectively, with the lowest amount of adhesive used. The sample ductility is also reduced with the lowest amounts of adhesive (0.5 mm and 1.0 mm adhesive) compared to the reference level (1.5 mm adhesive). Both levels also show a similar maximum displacement (Fig.

1 3b). This can be attributed to a change from adhesive-dependent behaviour (i.e., the adhesive provides
2 higher ductility and strength) to a core/skin-dependent behaviour with less adhesive. Similar features
3 are also present during the impact tests, with a consistent reduction in maximum load and quasi-constant
4 impact duration for less adhesive (Fig. 3d).

5

6

Table 3. Average results and standard deviations (in parentheses) of the flexural test.

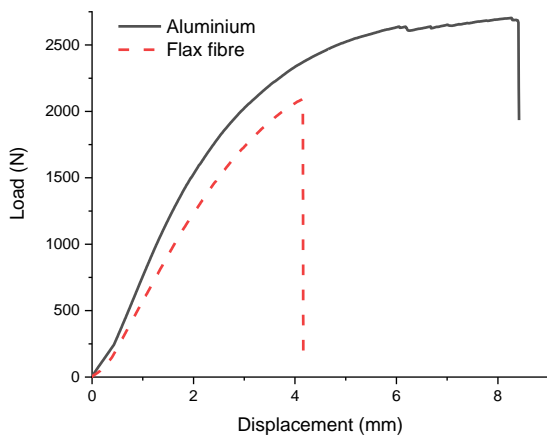
Conditions	Absolute Properties					Specific Properties			
	σ_{skin} [MPa]	τ_{core} [MPa]	G_{core} [MPa]	E_{flex} [GPa]	ρ [kg/m ³]	σ_{spec} [10 ³ Pa ^{1/2} .m ³ /g]	τ_{spec} [10 ³ Pa ^{1/2} .m ³ /g]	G_{spec} [10 ² Pa ^{1/3} .m ³ /g]	E_{spec} [10 ² Pa ^{1/3} .m ³ /g]
C1: Al_{0.5}+EP_{1.5}	158.1 (2.8)	1.1 (0.02)	28.5 (0.1)	2.9 (0.02)	549.5 (1.2)	22.9 (0.2)	1.9 (0.01)	5.6 (0.01)	26.0 (0.01)
C2: Al_{0.5}+EP_{1.0}	122.1 (3.6)	0.8 (0.02)	21.1 (0.01)	2.5 (0.02)	495.8 (6.3)	22.3 (0.6)	1.8 (0.05)	5.6 (0.07)	27.2 (0.3)
C3: Flax_{0.5}+EP_{1.5}	116.3 (8.8)	0.8 (0.06)	29.2 (2.0)	2.4 (0.2)	470.9 (9.6)	22.9 (0.6)	1.9 (0.05)	6.5 (0.10)	28.5 (0.4)
C4: Flax_{0.5}+EP_{1.0}	81.3 (3.1)	0.5 (0.02)	18.5 (0.8)	1.8 (0.1)	397.8 (2.9)	22.7 (0.4)	1.8 (0.03)	6.6 (0.05)	30.6 (0.4)
C5 (Extra): Flax_{0.5}+EP_{0.5}	62.9 (3.6)	0.4 (0.02)	15.5 (0.3)	1.6 (0.1)	323.8 (3.5)	24.5 (0.4)	2.0 (0.04)	7.7 (0.03)	36.1 (0.1)

7

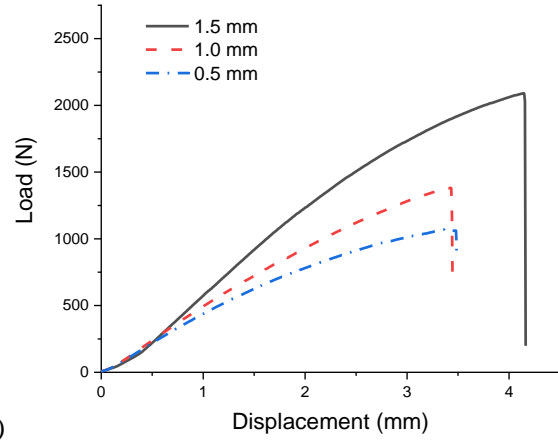
8

Table 4. Average results and standard deviations (in parentheses) from the drop-tower tests results.

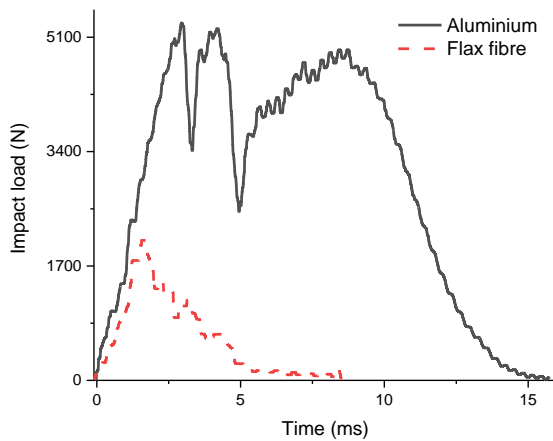
Conditions	Absolute Properties			Specific Properties	
	P_{max} [kN]	W_{abs} [J]	W_{ratio} [%]	P_{max} [N.m ³ /kg]	W_{spec} [10 ⁻³ N.m ⁴ /kg]
C1: Al_{0.5}+EP_{1.5}	4.6 (0.5)	51.3 (2.3)	95.2 (2.5)	8.3 (0.7)	89.3 (6.4)
C2: Al_{0.5}+EP_{1.0}	3.9 (0.1)	52.0 (1.1)	94.2 (0.6)	7.9 (0.1)	105.6 (0.7)
C3: Flax_{0.5}+EP_{1.5}	1.9 (0.1)	13.8 (1.2)	25.9 (2.1)	4.2 (0.1)	28.8 (2.3)
C4: Flax_{0.5}+EP_{1.0}	1.5 (0.2)	10.2 (0.1)	19.0 (0.1)	3.8 (0.3)	26.3 (0.5)
C5 (Extra): Flax_{0.5}+EP_{0.5}	1.0 (0.1)	7.5 (0.5)	14.1 (1.0)	3.0 (0.3)	22.4 (1.0)



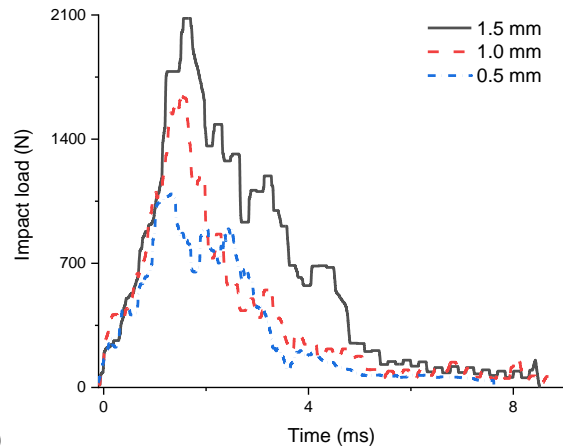
(a)



(b)



(c)



(d)

Figure 3. Force vs. displacement curves of the flexural tests and force vs. time curves of impact tests for both skins (a, c) and amounts of adhesive with flax samples (b, d), respectively.

3.1. Flexural tests

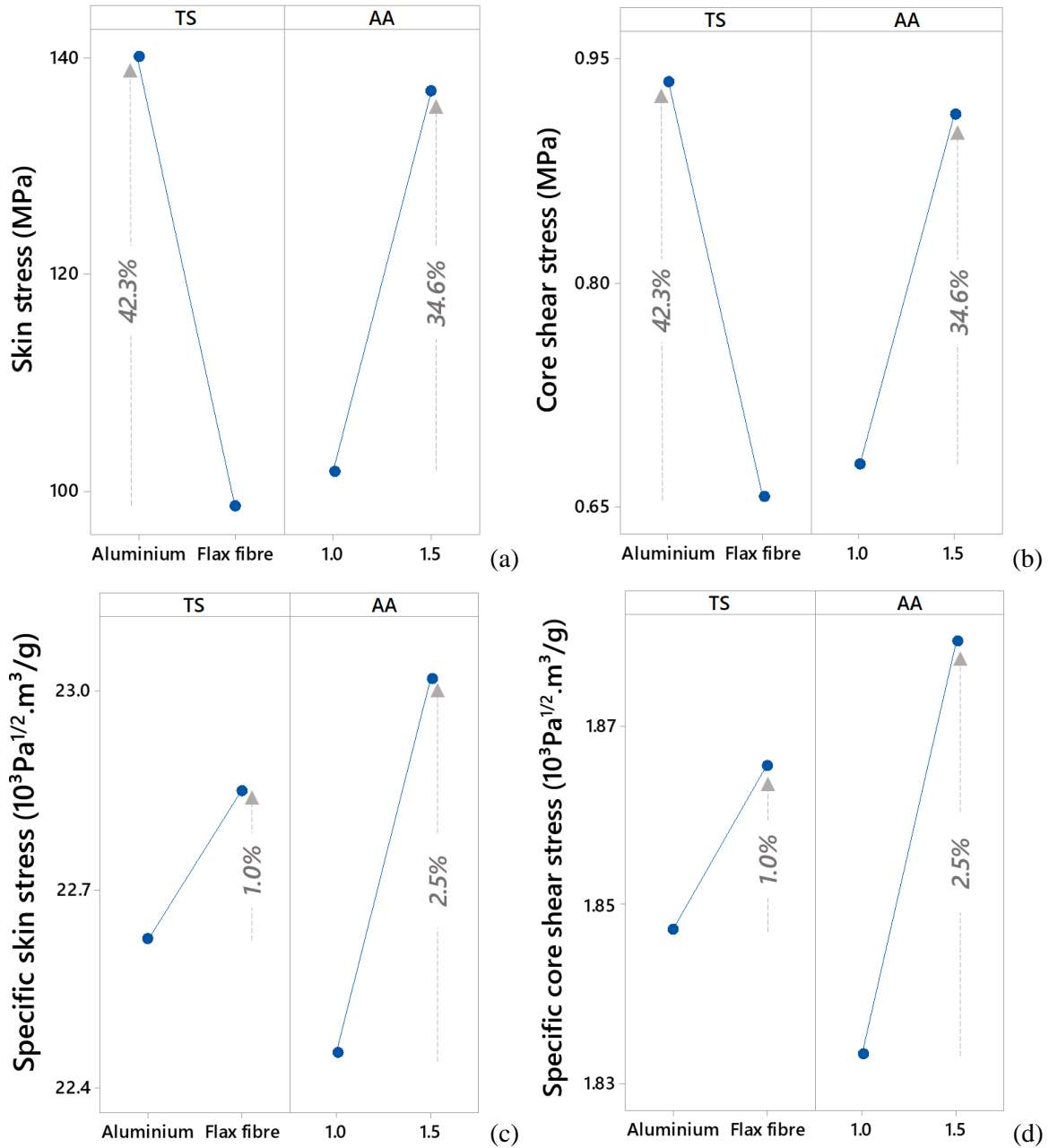
The results from the statistical analysis of the 2^2 full factorial design on the 3PB tests considering adhesive thickness levels of 1.5 and 1.0 mm are shown in Table 5. P-values less than or equal to 0.05 indicate that a factor or an interaction of factors is significant to affect the investigated response within a 95% confidence interval [39]. Table 5 confirms the significant influence of the type of skin on the investigated properties. In addition, the amount of adhesive significantly affects all absolute and specific flexural properties, except for the specific core shear modulus. The absolute core shear modulus, on the other hand, is the only response affected by the interaction between the ‘Type of skin’ and ‘Adhesive amount’ factors. The significant factors and the interaction analysed using statistical plots (Fig. 4 to 6) are underlined. The observed data show a satisfactory adjustment to the statistical model with R^2 (adj) close to 100% (between 90.14 and 99.95%) [39]. The data also follow the normal distribution by Anderson-Darling P-values above 0.05, which confirms the analysis of variance (ANOVA) conclusions [39].

1

Table 5. Analysis of variance (ANOVA) of the 2² factorial design for flexural test.

DoE factors and interaction		σ_{skin}	τ_{core}	G_{core}	E_{flex}	σ_{spec}	τ_{spec}	G_{spec}	E_{spec}
P-value ≤ 0.05	Type of skin (TS)	<u>0.000</u>	<u>0.000</u>	0.000	<u>0.000</u>	<u>0.041</u>	<u>0.041</u>	<u>0.000</u>	<u>0.000</u>
	Adhesive amount (AA)	<u>0.000</u>	<u>0.000</u>	0.000	<u>0.000</u>	<u>0.002</u>	<u>0.002</u>	0.479	<u>0.004</u>
	TS* AA	0.744	0.744	<u>0.000</u>	0.072	0.249	0.249	0.637	0.247
R ² -adj		98.57	98.57	99.95	99.83	90.14	90.14	97.31	96.08
Anderson Darling (P-value ≥ 0.05)		0.747	0.747	0.184	0.255	0.923	0.923	0.390	0.874

2



3

4

5

6

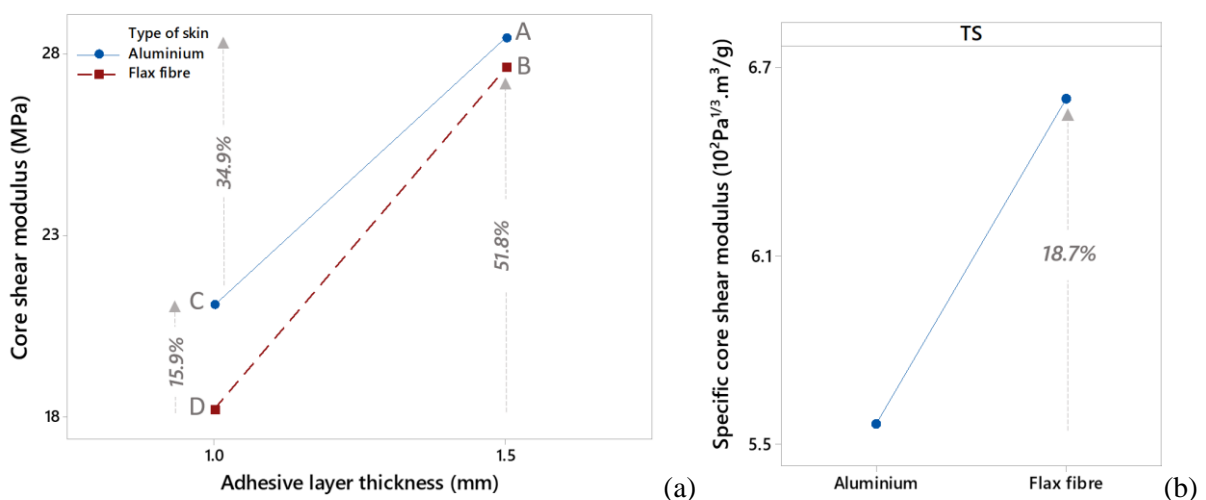
7

Figure 4. Main effect plots for skin stress and core shear stress (a, b) and their specific properties (c, d).

1 The strength-related properties from the 3PB test (i.e., the core shear and skin stresses) are shown
 2 in Figure 4, with their absolute and specific values. The behaviour of the two properties is similar, since
 3 they are directly dependent on the maximum flexural load at failure. The replacement of aluminium skin
 4 with flax fibre laminates reduces the maximum stress on skin and core by 29.7%. A similar reduction
 5 occurs with a smaller amount of adhesive – 25.7%. The less adhesive amount has been identified in
 6 previous work as the cause of reduced mechanical properties. The adhesive flows around the cap walls,
 7 promoting bonding between adjacent caps and preventing buckling of the wall. The lower amount of
 8 adhesive reduces the support of the thermoplastic core (the bottle cap) with the stiff polymeric matrix.
 9 In addition, less adhesive reduces the adequate adhesion to the skin [34]. However, the specific
 10 properties indicate that a moderate 2.5% increment is obtained by reducing the quantity of adhesive and
 11 by using natural fibre-based skin; this indicates a similar mechanical efficiency provided by the natural
 12 fibres with a lower density adhesive. The panel density is 29% lower with the use of flax skin and less
 13 adhesive amount, which mitigates the reductions in properties and improves mechanical efficiency.

14 The shear stiffness (absolute and specific) of the core is significantly affected by the interaction
 15 of the factors (Table 5), as also shown in Figure 5. A higher amount of adhesive increases the core shear
 16 modulus by 52% when flax fibre skins are used, while aluminium-based panels are less sensitive to the
 17 increase in the bonding layer. Fisher’s test, for comparison of means, is conducted for the absolute core
 18 modulus to identify which interactions are significantly different from each other [39]. The test attributes
 19 different letters when the means are significantly distinct within a 95% confidence interval, as shown in
 20 Figure 5a. Fisher’s test shows that the skin type significantly affects the core modulus at both levels of
 21 adhesive amount. The use of aluminium skins combined with less adhesive amount leads to a 16%
 22 higher core shear modulus than flax panels. A minor increase in shear modulus (~3%) at the 1.5 mm
 23 adhesive layer level is evident, which shows that the panel is less sensitive to changes in the skin at this
 24 level. An opposite behaviour is found for the specific core shear modulus, which has an 18.7% larger
 25 modulus with flax fibre skins. This property is not affected by the amount of adhesive (Table 5).

26



27

28 Figure 5. Interaction and main effect plots for core shear modulus (a) and its specific modulus (b).

The flexural modulus is affected by individual factors, as shown in Figure 6. A higher absolute modulus is observed for panels made with aluminium skins and 1.5 mm adhesive layer thickness, with increments of up to 31%. It is noteworthy that the specific properties evidence the advantage of a lightweight design, with increases in the mechanical efficiency of the panel by 11.3% and 5.6% when considering flax fibres skins and less adhesive, respectively.

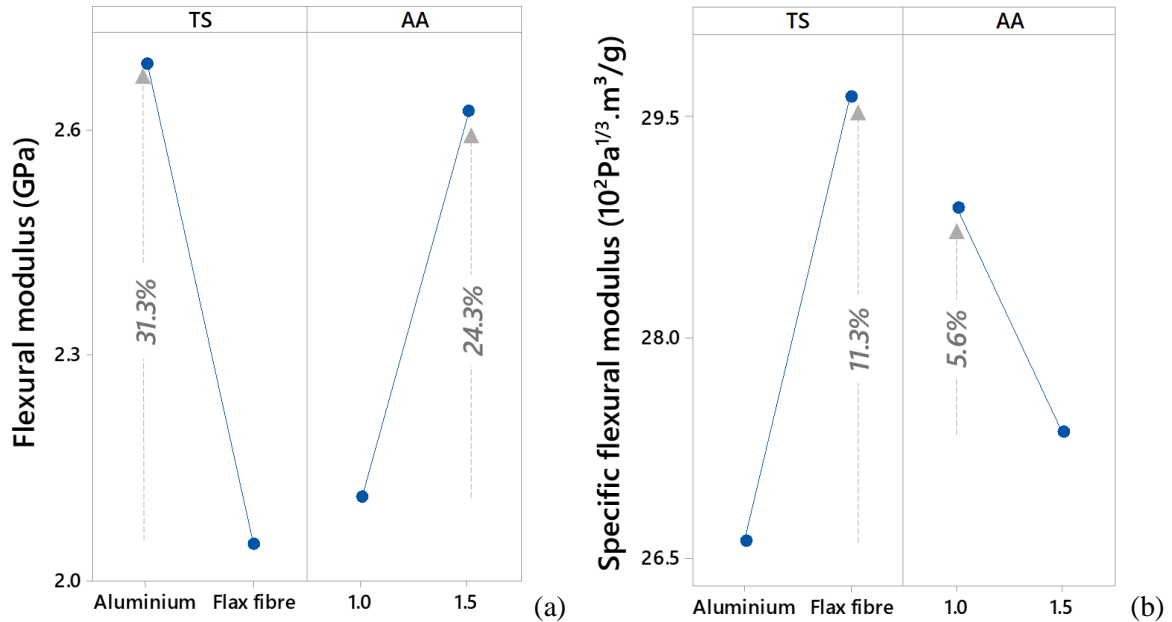


Figure 6. Main effect plots for flexural modulus (a) and its specific property (b).

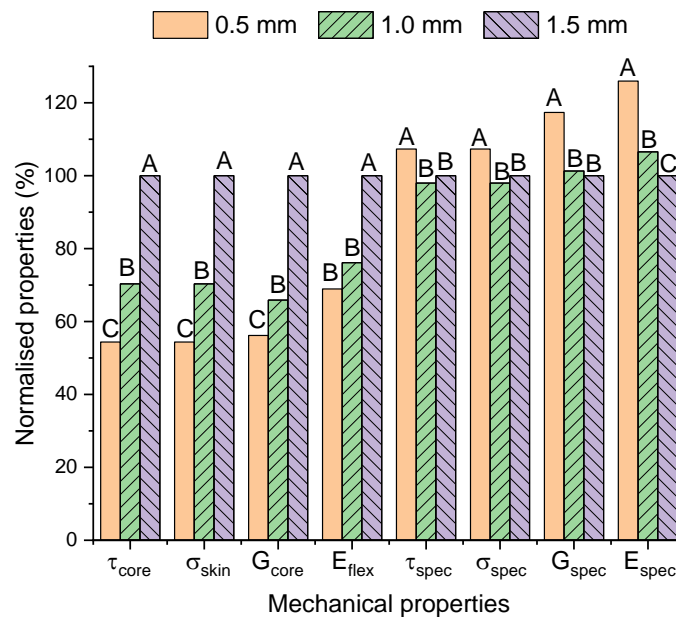
The contribution of the adhesive reduction is further investigated by an extra condition made with an adhesive layer thickness of 0.5 mm. This analysis is considered since most of the properties assessed in this study are affected by the amount of adhesive, regardless of the skin type. Therefore, only the skin with the highest specific properties (in this case, the lightweight skin made of flax fibres) is investigated in the second experiment. The results of the analysis of variance (ANOVA) are shown in Table 6. The adhesive thickness of 0.5 mm significantly affects all the investigated responses, including the specific core shear modulus. To complement ANOVA, Fisher's test is performed to verify which means are significantly different by assigning different group of letters. The normalised results to the reference condition (the panel with 1.5 mm adhesive layer) and the Fisher's test groups are shown in Figure 7.

Table 6. Analysis of variance (ANOVA) for independent flexural test of adhesive thickness.

Independent factor	σ_{skin}	τ_{core}	G_{core}	E_{flex}	σ_{spec}	τ_{spec}	G_{spec}	E_{spec}
Adhesive thickness	<u>0.001</u>	<u>0.001</u>	<u>0.000</u>	<u>0.002</u>	<u>0.002</u>	<u>0.002</u>	<u>0.002</u>	<u>0.001</u>
R ² -adj	98.07	98.07	99.81	97.38	97.55	97.55	97.34	98.90

Figure 7 shows that the absolute properties are higher with thicker adhesive layers (Group A), as indicated in the previous study, which tested two levels of adhesive amount (0.8 and 1.5 mm) [34]. The

1 reduction of the adhesive layer from 1.0 to 0.5 mm reduces the stresses of the skins and the core by 30%
 2 and 46% (Groups B and C), respectively. This indicates that the losses of mechanical strength do not
 3 follow a linear relationship with the reduction of the adhesive layer, reaching a moderate intensity with
 4 further reductions in the polymer amount. This trend is most evident for the core shear and flexural
 5 moduli, which show closer results between the intermediate and the lowest adhesive amounts. Fisher's
 6 test reveals that, for the flexural modulus, panels with adhesive layers of 1.0 and 0.5 mm have similar
 7 stiffness (Group B), only distinguishable from the panel with the greatest adhesive amount (Group A).
 8 The similarity implies a change in the behaviour of panels made with thinner adhesive thickness. The
 9 benefits of reducing adhesive amounts are shown in the specific properties. The statistical analysis
 10 shows similar efficiency of both configurations analysed previously (1.0 and 1.5 mm adhesive layer)
 11 with a moderate increase in properties with a smaller adhesive amount. A similar result was found in
 12 the previous study with the bottle caps core [34]. The results obtained by the lowest adhesive amount,
 13 however, reveal a significant benefit for the panel efficiency. Fisher's test indicates the 0.5 mm thick
 14 adhesive layer (Group A) is 7.3% stronger and up to 26% stiffer compared to other conditions, which
 15 present similar results for skin stress, core shear stress, and core shear modulus (Group B).



16
 17 Figure 7. Normalised mechanical properties for the independent test with flax fibres.

18
 19 **3.2. Impact test**

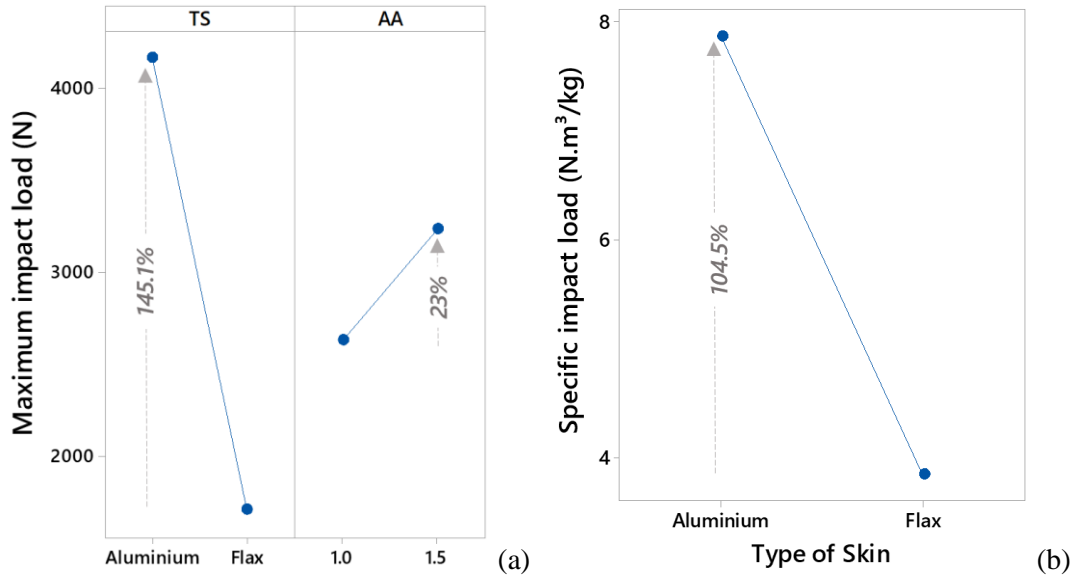
20 Table 7 shows the statistical analysis for low-velocity impact tests. The maximum impact load
 21 and the energy absorption properties are affected by the main factors, while the specific energy
 22 absorption is affected by its interaction, presenting P-Values below 0.05 [39]. The P-Values underlined
 23 in Table 7 correspond to the analysed effects shown in Figures 8 and 9. The statistical models also show
 24 good correlations with the experimental data, exhibiting R^2 (adj) above 97.47%. The normality of the
 25 data is verified by Anderson-Darling with P-Values above 0.05, validating ANOVA [39].
 26

1

Table 7. Analysis of variance (ANOVA) of the 2² factorial design for impact test.

DoE factors and interaction		P_{max}	W_{abs}	W_{ratio}	P_{spec}	W_{spec}
P -Value ≤ 0.05	Type of skin (TS)	<u>0.000</u>	<u>0.000</u>	<u>0.000</u>	<u>0.000</u>	0.000
	Adhesive amount (AA)	<u>0.017</u>	0.118	<u>0.010</u>	0.285	0.011
	TS * AA	0.919	0.197	0.115	<u>0.287</u>	<u>0.003</u>
R^2 -adj		97.47	99.70	99.90	98.34	99.56
Anderson Darling (P-value ≥ 0.05)		0.542	0.631	0.816	0.344	0.832

2

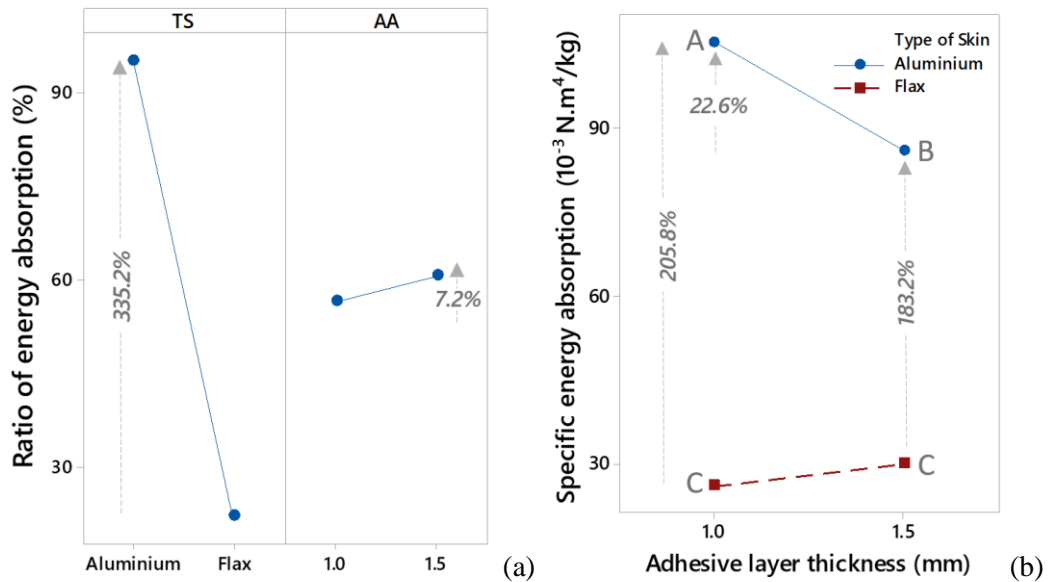


3

Figure 8. Main effect plots for absolute (a) and specific impact load (b).

4

5



6

Figure 9. Interaction plots for energy absorption ratio (a) and specific energy absorption (b).

7

8

9

10

The maximum load is affected individually by both factors investigated, while the specific load is affected only by the type of skin (Table 7). Aluminium skins increase the maximum load by 145%

1 due to the greater strength and ductility of the metallic skin compared to the flax fibre laminates. This
 2 effect is also observed in the specific impact load, which is 104.5% higher for aluminium skins than for
 3 flax skins. The greater amount of adhesive also increases the absolute maximum load by 23% (Fig. 8a).
 4 This increment is not seen in a specific response. A higher density of panels made with a thicker adhesive
 5 layer lessens the increase in mechanical resistance when considering the specific performance of the
 6 sandwich panels. The quantity of adhesive used, therefore, has a limited influence on the mechanical
 7 efficiency of the panels under impact.

8 The greater ductility and mechanical resistance of aluminium skins also affect the energy
 9 absorption capacity of sandwich panels. The ratio of absorbed energy to total energy represents the
 10 efficiency of the structure in absorbing energy during impact and is shown in the main effect plot in
 11 Figure 9a. Fisher's test groups are also shown in the interaction plot for specific energy absorption (Fig.
 12 9b). Aluminium-based panels reach energy absorption efficiencies up to 335% higher than flax-based
 13 panels. Unidirectional flax skins exhibit a rapid transversal rupture of the matrix-fibre bonding after the
 14 impact event, which significantly reduces the energy absorption capacity during low-velocity impact
 15 tests, as described in section 3.4. The greater amount of adhesive also increases the energy absorption
 16 ratio by 7.2%. However, the use of a thicker adhesive layer (1.5 mm adhesive) reduces the specific
 17 energy absorption of panels made with aluminium skins by 18.4% (Groups A and B – Fig. 9b), while
 18 the flax-based samples are similarly efficient for both levels (Group C). Aluminium skins increase the
 19 specific energy absorption of the sandwich panel by up to 206% compared to composite-based samples.

20 The results of the independent test considering a thinner thickness of adhesive on flax composite
 21 skins are shown in Table 8 and Figure 10. ANOVA (P-values ≤ 0.05) shows that all properties are
 22 affected by the amount of adhesive, with high predictability of the models (R^2 above 91.00%). Figure
 23 10 shows the normalised properties to the reference condition (1.5 mm adhesive layer) considering three
 24 levels of thickness of the adhesive layer. Fisher's test reveals that the additional level (0.5 mm) for
 25 adhesive thickness affects all investigated responses, with reductions of 31% for the specific maximum
 26 load and of 26.2% for the specific energy absorption. The absolute properties show substantial
 27 reductions of up to 53.5% for 0.5 mm adhesive layer panels. The intermediate level (1.0 mm) also shows
 28 a significant reduction of the impact load and energy absorption. The reduction in the amount of
 29 adhesive limits the feasibility of using unidirectional flax fibres as skins in sandwich panels subject to
 30 impact loads. In comparison with alternative sustainable skins presented in the previous study, such as
 31 recycled PET foil [5], however, these findings indicate a significant increase of ~13% in the performance
 32 of the panel due to the greater mechanical strength of skins composed of flax fibre composites.

34 Table 8. Analysis of variance (ANOVA) for independent impact test of adhesive thickness.

Independent factor	P_{max}	W_{abs}	W_{ratio}	P_{spec}	W_{spec}
Adhesive thickness	<u>0.005</u>	<u>0.008</u>	<u>0.007</u>	<u>0.007</u>	<u>0.013</u>
R^2 -adj	95.26	93.50	94.13	93.91	91.00

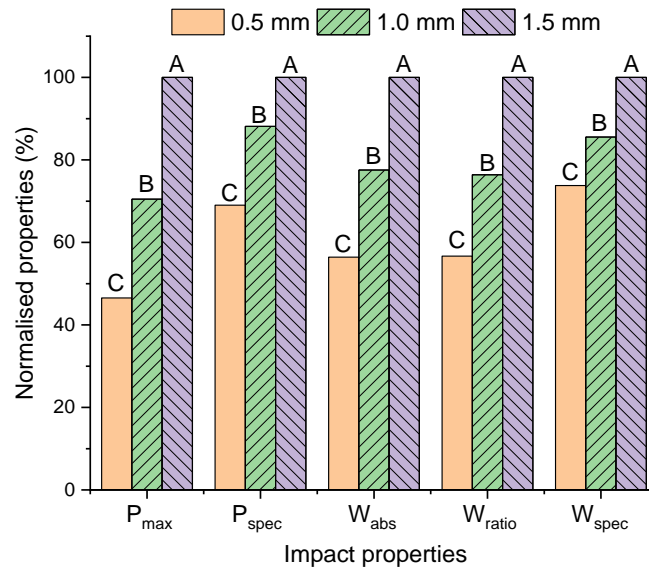
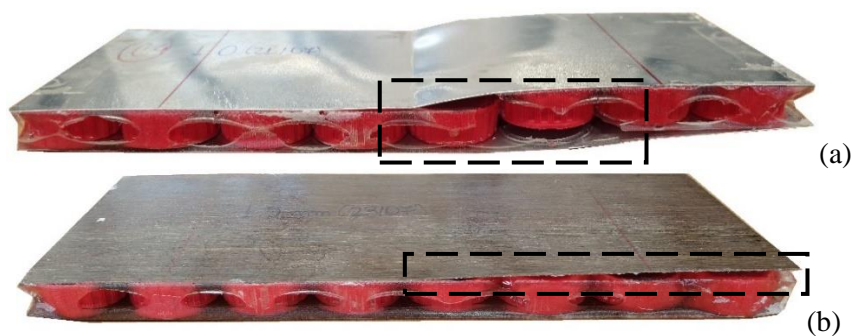


Figure 10. Normalised impact properties for the independent test with flax fibres.

3.3. Failure mode

Figure 11 shows the main failure modes of the sandwich panels under bending and impact tests. The samples made with aluminium skins have the typical failure described in previous studies [5,33–35], characterised by the shear sliding of the adjacent bottle caps, leading to localised debonding of the skin to the adhesive layer (Fig. 11a). Samples with flax fibres also fail to adhere to the adhesive. The sudden drop in the force vs displacement curves is caused by the rapid propagation of debonding between the skin and the adhesive layer (Fig. 11b). In addition, a small damage to the core is observed in the centre of the panels made with a greater amount of adhesive, but no visible debonding between the adjacent caps is identified. The reduction in the amount of adhesive, however, resulted in a core failure mode similar to that of the aluminium-based panel, which is caused by core damage. Failure under impact loads, on the other hand, is mainly influenced by the skins. Aluminium skins show considerable deformation under impact and partial debonding of the core (Fig. 11c), but no rupture is identified in these samples. This skin contributes to a greater energy absorption with a moderate rebound of the impactor. Samples with unidirectional flax fibres show a full rupture of the skin, which leads to the propagation of cracks longitudinally to the fibre direction, from the central cap to the edges of the sample (Fig. 11d). The impactor fully perforates the sample, limiting the energy absorption capacity of the flax-based panel made of unidirectional laminates.



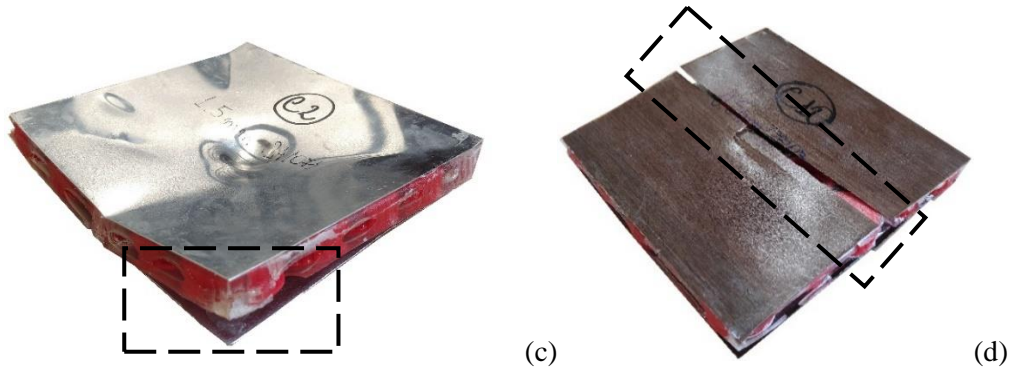


Figure 11. Failure mode of aluminium (a, c) and flax-based panels (b, d) under flexural and impact, respectively.

3.4. FE results and optimisation

The results of the finite element simulations are shown in Figures 12 and 13. The material properties of the models developed in the LS-Dyna are shown in Table 9. The properties are based on the mechanical properties listed in Table 1 and on the results obtained in previous works [25,33]. The properties of the laminate normal to the fibre direction, required for the Chang-Chang model describing flax laminates, are obtained with the micromechanical analysis of unidirectional flax laminates, as described by Oliveira et al. [27]. The failure of flax laminates is based on the effective failure strain determined experimentally [38]. A satisfactory convergence is achieved between the experimental and simulation data, especially for the quasi-static analysis of the sandwich panels with a skin shell mesh of 36×12 elements. The impact models have a mesh of 20×20 elements on the skin. The solid elements of the core are of 4 mm size. The mechanical properties and failure strains are based on the component's characterisation (Table 1), achieving a good correlation between the experimental load curves and FE.

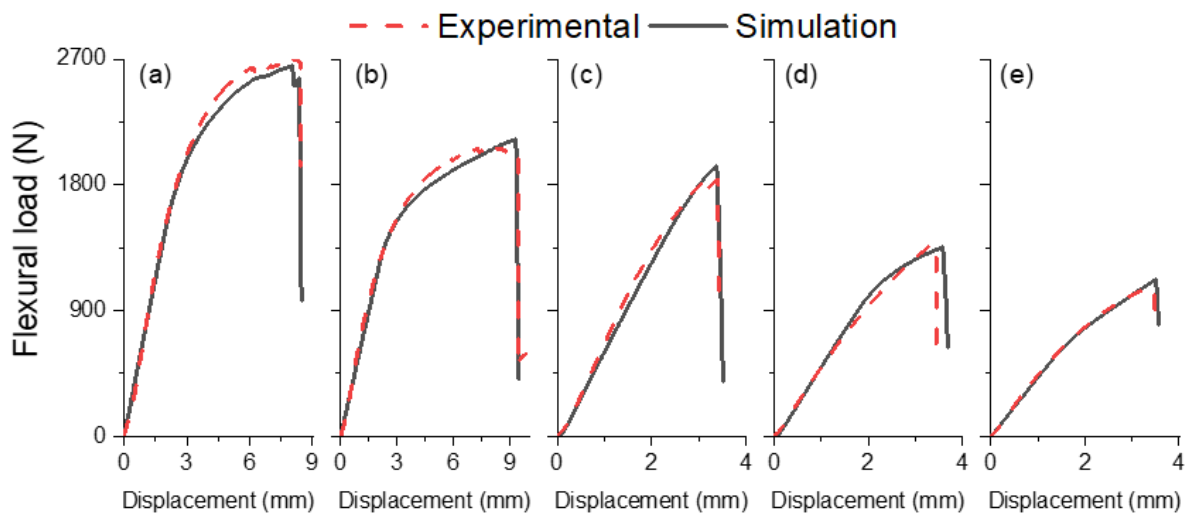


Figure 12. Force vs displacement results of quasi-static experiment and FE models for the conditions 1 to 5 (a - e, respectively).

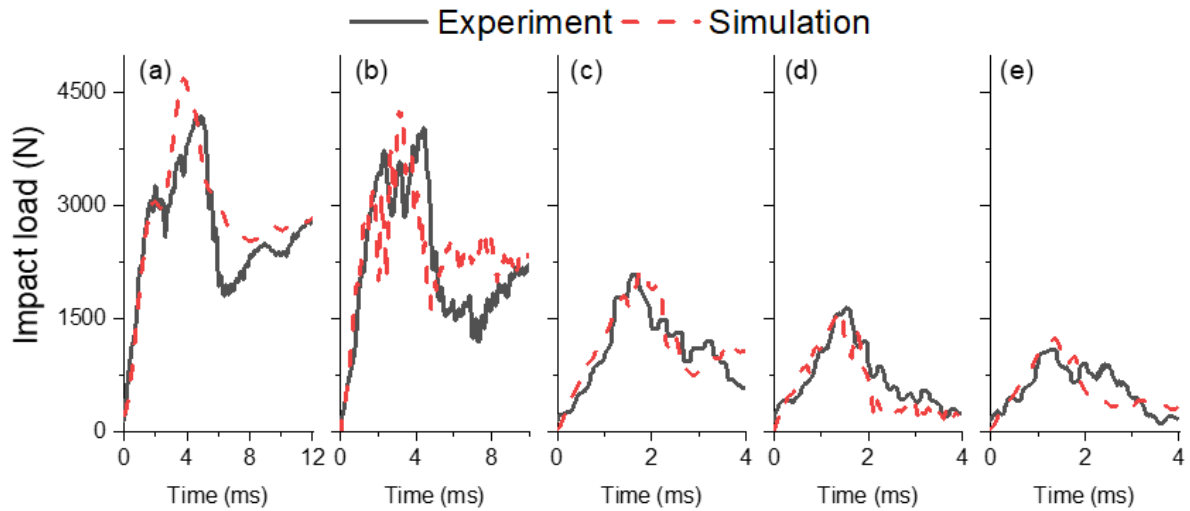


Figure 13. Force vs time results of dynamic experiment and FE models for the conditions 1 to 5 (a - e, respectively).

Table 9. Modelling parameters for the different components of the sandwich panels.

Components	MAT-024/054 main parameters					
	Density [kg/m ³]	Young's Modulus [GPa]	Poisson's ratio	Yield stress [MPa]	Tangent Modulus [GPa]	Plastic strain to failure
Aluminium skin	2720	70.5	0.3	165.0	2.0	0.16
Bottle caps core	1.5 mm adhesive	1200	1.9	23.0	0.4	0.06
	1.0 mm adhesive	1200	1.4	19.0	0.1	0.03
	0.5 mm adhesive	1200	1.0	8.0	0.4	0.02
Flax composite (MAT-054) (adapted from [27])	Density [kg/m ³]	E ₁ [GPa]	E ₂ = E ₃ [GPa]	G ₁₂ [GPa]	Poisson's ratio	Effective failure strain
	1200	35.6	4.4	4.29	0.33	0.02

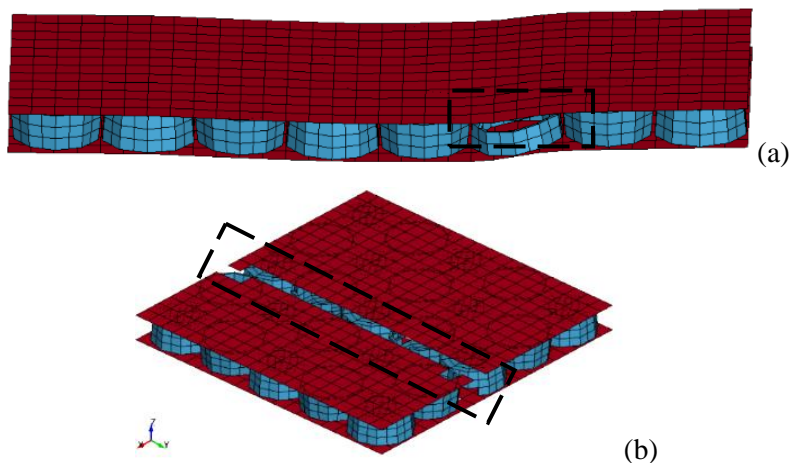


Figure 14. Failure of samples obtained via FEA for conditions C3 for quasi-static (a) and dynamic test (b).

The results from the FE models show a satisfactory agreement with the experimental ones. They further confirm that the behaviour of the sandwich panel is more dependent on the individual

1 performance of plastic caps and aluminium/flax skins when less amount of adhesive (equivalent to 0.5
 2 mm thick adhesive layer) is used compared to the largest amount of adhesive investigated (equivalent
 3 to 1.5 mm layer). The FE model also captures the failure of the sandwich panel based on the debonding
 4 of the adhesive layer between the skin and the core for quasi-static testing by failure of the core elements
 5 adjacent to the skin. The rupture of the skin is also observed in the panels tested under the impact via
 6 drop tower by matrix failure between the fibres. The failure mode predicted by the FE models for both
 7 tests is shown in Figure 14.

8 The dynamic properties of sandwich panels with flax laminate as skins are limited by the rapid
 9 matrix failure of the UD stacking sequence investigated in this study. A preliminary optimisation of the
 10 sandwich panel is developed using the calibrated FE models, investigating the effect of the skin
 11 thickness (0.5, 1.5 and 2.5 mm) and the direction of flax fibre laminates on the response of the sandwich
 12 panels. The different stacking sequences investigated for the thicker laminates are shown in Table 10.
 13 The stacking sequences investigated aim to determine the effect of different fibre orientations on the
 14 impact resistance and energy absorption for the future experimental investigation of woven flax
 15 laminates. The results for the 3-point bending and drop tower models are shown in Table 10 and Figure
 16 15. Thicker flax samples increase the panel density by 43.7%, while the maximum impact load and
 17 energy absorption are 126% and 108% larger with 2.5 mm unidirectional flax laminates, respectively.
 18 The increase in flexural load with thicker skins is, however, limited to 41%. The change in fibre direction
 19 affects the static load only by up to 3% for each thickness. It is noteworthy that the main effect of the
 20 different fibre directions is observed in the dynamic properties of the flax-based panel. Moderate
 21 increments of up to 12% are found for maximum impact load, especially for bidirectional laminates.
 22 Energy absorption, however, shows a significant increase of 22 and 28% with multidirectional laminate
 23 skins of 1.5 and 2.5 mm, respectively. The significant increase in energy absorption is explained by the
 24 mechanical plots in Figure 15.b. The bending properties are barely affected by the change in the fibre
 25 direction, while the impact loads show an increase in the second peak in the force vs time curves of the
 26 thicker samples, especially in the bidirectional laminates. This second peak is associated with an
 27 improvement in the response of the lower skin, which presents greater resistance to rupture due to the
 28 thicker laminate and the energy absorption of the upper skin, reducing the overall damage of the sample.

29

30 Table 10. Mechanical properties of sandwich panels with increased thickness and fibre orientation.

Flax skin thickness	Fibre direction	Equivalent density (kg/m ³)	Bending load (N)	Maximum load (N)	Energy absorption (J)
0.5 mm	[0] ₃	470.9	1,908.45	1,994.06	13.8
1.5 mm	[0] ₉	589.7	2,105.26	2,905.34	22.1
	[0 ₃ /90 ₃ /0 ₃]		2,159.09	3,198.10	27.0
2.5 mm	[0] ₁₅	676.5	2,711.17	4,521.72	28.8
	[0 ₅ /90 ₅ /0 ₅]		2,734.48	5,078.84	36.1
	[0 ₃ /-45 ₃ /90 ₃ /45 ₃ /0 ₃]		2,699.33	4,824.58	36.8

31

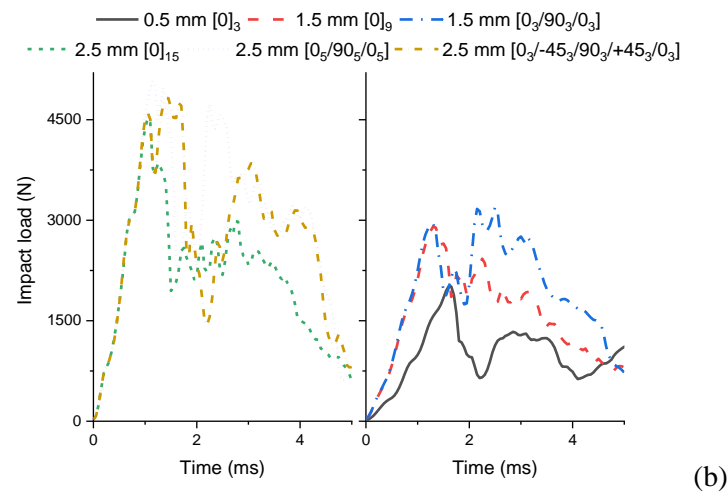
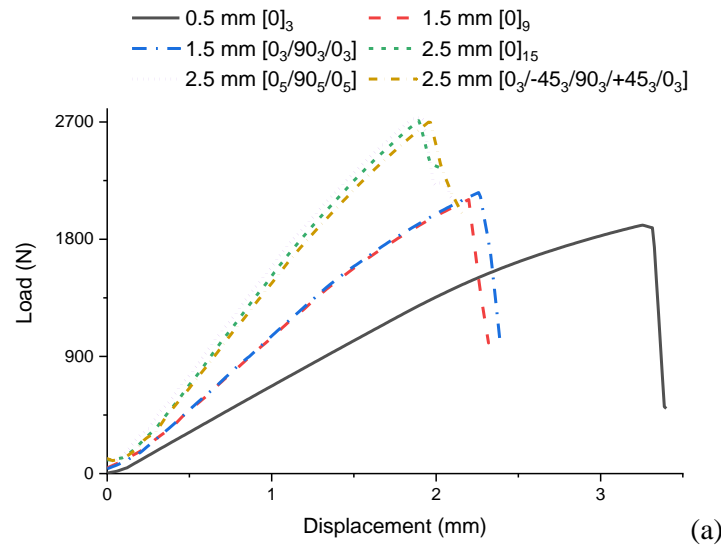


Figure 15. Quasi-static (a) and dynamic (b) response of model with thicker multidirectional laminates.

4. CONCLUSIONS

This work investigates the use of flax-fibre laminates as skin for an eco-friendly sandwich panel based on upcycled bottle caps as a honeycomb core compared to metallic skins. The effects of the amount of adhesive are also studied. The main conclusions of this work are described below:

- i. Flax fibre skins with $[0]_3$ stacking sequence reduce absolute mechanical strength and stiffness under flexural loads by 42 and 31%, respectively, while increasing specific quasi-static properties by up to 19% due to their lightweight design.
- ii. The reduction of the thickness of the adhesive layer decreases the absolute mechanical properties under bending and low-velocity impact by 34% and 49%, respectively. The lower quantity of adhesive used however provides a significant 26% increase of the specific flexural properties; the specific impact properties do not benefit from using a lower adhesive amount.
- iii. The energy absorption under impact is mainly affected by the type of skin, in which the aluminium-based structures have almost 95% energy absorption efficiency for a greater amount

1 of adhesive. The use of UD flax and the lowest adhesive amount reduces the energy absorption
2 by 77%.

3 iv. Finite element models show a satisfactory adjustment of the quasi-static and dynamic
4 responses of the sandwich panels with flax skins and lower amounts of adhesive. A proposed
5 modification of the laminate configuration with thicker multidirectional laminates shows an
6 increase of up to 166% in energy absorption compared to UD flax laminates.

7 The use of natural fibres as a replacement for aluminium skin is a highly promising approach to
8 further reduce the environmental impact associated with the upcycled bottle cap sandwich panel. The
9 limited bonding to the adhesive skin and the reduced resistance against low-velocity impact by UD fibre
10 laminates can be improved by using alternative adhesive formulations (e.g. bio-based polyurethane) and
11 alternative fibre orientations (e.g. $[\pm 45^\circ]$), as indicated by the preliminary FE models. The components
12 described in this work can be used to design an eco-friendly and low carbon footprint structure with
13 good mechanical performance.

14 15 **ACKNOWLEDGEMENTS**

16 The authors acknowledge the support of CNPq-Brazil (PhD Scholarship 290224/2017-9, PQ -
17 309885/2019-1) in this study.

18 19 **REFERENCES**

20 [1] Schönmayr D. Automotive recycling, plastics and sustainability: The recycling renaissance. Cham:
21 Springer International Publishing; 2017.

22 [2] Kim J-K, Yu T-X. Forming and failure behaviour of coated, laminated and sandwiched sheet
23 metals: a review. *Journal of Materials Processing Technology* 1997;63(1-3):33–42.
24 [https://doi.org/10.1016/s0924-0136\(96\)02596-4](https://doi.org/10.1016/s0924-0136(96)02596-4).

25 [3] Bitzer T. Honeycomb Technology: Materials, Design, Manufacturing, Applications and Testing.
26 Dordrecht, s.l.: Springer Netherlands; 1997.

27 [4] Civancik-Uslu D, Ferrer L, Puig R, Fullana-I-Palmer P. Are functional fillers improving
28 environmental behavior of plastics? A review on LCA studies. *Sci Total Environ* 2018;626:927–40.
29 <https://doi.org/10.1016/j.scitotenv.2018.01.149>.

30 [5] Oliveira PR, May M, Panzera TH, Scarpa F, Hiermaier S. Improved sustainable sandwich panels
31 based on bottle caps core. *Composites Part B: Engineering* 2020:108165.
32 <https://doi.org/10.1016/j.compositesb.2020.108165>.

33 [6] Mohanty A, Misra M, Drzal L (eds.). *Natural Fibers, Biopolymers, and Biocomposites*. CRC Press;
34 2005.

- 1 [7] Hoto R, Furundarena G, Torres JP, Muñoz E, Andrés J, García JA. Flexural behavior and water
2 absorption of asymmetrical sandwich composites from natural fibers and cork agglomerate core.
3 *Materials Letters* 2014;127:48–52. <https://doi.org/10.1016/j.matlet.2014.04.088>.
- 4 [8] Vinayagamoorthy R, Rajeswari N. Mechanical performance studies on *Vetiveria zizanioides*
5 /jute/glass fiber-reinforced hybrid polymeric composites. *Journal of Reinforced Plastics and Composites*
6 2014;33(1):81–92. <https://doi.org/10.1177/0731684413495934>.
- 7 [9] Vieira LMG, dos Santos JC, Panzera TH, Rubio JCC, Scarpa F. Novel fibre metal laminate
8 sandwich composite structure with sisal woven core. *Industrial Crops and Products* 2017;99:189–95.
9 <https://doi.org/10.1016/j.indcrop.2017.02.008>.
- 10 [10] Rao S, Jayaraman K, Bhattacharyya D. Micro and macro analysis of sisal fibre composites hollow
11 core sandwich panels. *Composites Part B: Engineering* 2012;43(7):2738–45.
12 <https://doi.org/10.1016/j.compositesb.2012.04.033>.
- 13 [11] Ferreira BT, da Silva LJ, Panzera TH, Santos JC, Freire RTS, Scarpa F. Sisal-glass hybrid
14 composites reinforced with silica microparticles. *Polymer Testing* 2019;74:57–62.
15 <https://doi.org/10.1016/j.polymertesting.2018.12.026>.
- 16 [12] Liu T, Hou S, Nguyen X, Han X. Energy absorption characteristics of sandwich structures with
17 composite sheets and bio coconut core. *Composites Part B: Engineering* 2017;114:328–38.
18 <https://doi.org/10.1016/j.compositesb.2017.01.035>.
- 19 [13] Dutra JR, Moni Ribeiro Filho SL, Christoforo AL, Panzera TH, Scarpa F. Investigations on
20 sustainable honeycomb sandwich panels containing eucalyptus sawdust, Piassava and cement particles.
21 *Thin-Walled Structures* 2019;143:106191. <https://doi.org/10.1016/j.tws.2019.106191>.
- 22 [14] da Costa RRC, Sato ES, Ribeiro ML, Medeiros Rd, Vieira AFC, Guedes RM et al. Polyurethane
23 derived from castor oil reinforced with long cotton fibers: Static and dynamic testing of a novel eco-
24 friendly composite material. *Journal of Composite Materials* 2020;54(22):3125–42.
25 <https://doi.org/10.1177/0021998320911984>.
- 26 [15] Tita SPS, Medeiros R, Tarpani JR, Frollini E, Tita V. Chemical modification of sugarcane bagasse
27 and sisal fibers using hydroxymethylated lignin: Influence on impact strength and water absorption of
28 phenolic composites. *Journal of Composite Materials* 2018;52(20):2743–53.
29 <https://doi.org/10.1177/0021998317753886>.
- 30 [16] Oliveira PR, Ribeiro Filho SLM, Panzera TH, Christoforo AL, Durão LMP, Scarpa F. Hybrid
31 polymer composites made of sugarcane bagasse fibres and disposed rubber particles. *Polymers and*
32 *Polymer Composites* 2020;1:096739112094345. <https://doi.org/10.1177/0967391120943459>.

- 1 [17] Yan L, Chouw N, Jayaraman K. Flax fibre and its composites – A review. *Composites Part B: Engineering* 2014;56:296–317. <https://doi.org/10.1016/j.compositesb.2013.08.014>.
- 3 [18] Symington MC, Banks WM, West OD, Pethrick RA. Tensile Testing of Cellulose Based Natural
4 Fibers for Structural Composite Applications. *Journal of Composite Materials* 2009;43(9):1083–108.
5 <https://doi.org/10.1177/0021998308097740>.
- 6 [19] Sadeghian P, Hristozov D, Wroblewski L. Experimental and analytical behavior of sandwich
7 composite beams: Comparison of natural and synthetic materials. *Jnl of Sandwich Structures &*
8 *Materials* 2018;20(3):287–307. <https://doi.org/10.1177/1099636216649891>.
- 9 [20] Monti A, EL Mahi A, Jendli Z, Guillaumat L. Quasi-static and fatigue properties of a balsa cored
10 sandwich structure with thermoplastic skins reinforced by flax fibres. *Jnl of Sandwich Structures &*
11 *Materials* 2019;21(7):2358–81. <https://doi.org/10.1177/1099636218760307>.
- 12 [21] Prabhakaran S, Krishnaraj V, Shankar K, Senthilkumar M, Zitoune R. Experimental investigation
13 on impact, sound, and vibration response of natural-based composite sandwich made of flax and
14 agglomerated cork. *Journal of Composite Materials* 2020;54(5):669–80.
15 <https://doi.org/10.1177/0021998319871354>.
- 16 [22] Oliveira LÁd, Santos JCd, Panzera TH, Freire RTS, Vieira LMG, Rubio JCC. Investigations on
17 short coir fibre–reinforced composites via full factorial design. *Polymers and Polymer Composites*
18 2018;26(7):391–9. <https://doi.org/10.1177/0967391118806144>.
- 19 [23] Pizzi A, Mittal KL. *Handbook of Adhesive Technology, Revised and Expanded*. 2nd ed. Hoboken:
20 Taylor and Francis; 2003.
- 21 [24] da Costa RRC, Medeiros Rd, Ribeiro ML, Tita V. Experimental and numerical analysis of single
22 lap bonded joints: Epoxy and castor oil PU-glass fibre composites. *The Journal of Adhesion* 2017;93(1-
23 2):77–94. <https://doi.org/10.1080/00218464.2016.1172212>.
- 24 [25] Oliveira PR, May M, Panzera TH, Scarpa F, Hiermaier S. Reinforced biobased adhesive for eco-
25 friendly sandwich panels. *International Journal of Adhesion and Adhesives* 2020;98:102550.
26 <https://doi.org/10.1016/j.ijadhadh.2020.102550>.
- 27 [26] Li W-T, Long Y-L, Huang J, Lin Y. Axial load behavior of structural bamboo filled with concrete
28 and cement mortar. *Construction and Building Materials* 2017;148:273–87.
29 <https://doi.org/10.1016/j.conbuildmat.2017.05.061>.
- 30 [27] Ávila de Oliveira L, Coura GLC, PassaiaTonatto ML, Panzera TH, Placet V, Scarpa F. A novel
31 sandwich panel made of prepreg flax skins and bamboo core. *Composites Part C: Open Access*
32 2020;3:100048. <https://doi.org/10.1016/j.jcomc.2020.100048>.

- 1 [28] Grünewald J, Parlevliet P, Altstädt V. Manufacturing of thermoplastic composite sandwich
2 structures. *Journal of Thermoplastic Composite Materials* 2017;30(4):437–64.
3 <https://doi.org/10.1177/0892705715604681>.
- 4 [29] Hassan MZ, Umer R, Balawi S, Cantwell WJ. The impact response of environmental-friendly
5 sandwich structures. *Journal of Composite Materials* 2014;48(25):3083–90.
6 <https://doi.org/10.1177/0021998313506727>.
- 7 [30] Cabrera NO, Alcock B, Peijs T. Design and manufacture of all-PP sandwich panels based on co-
8 extruded polypropylene tapes. *Composites Part B: Engineering* 2008;39(7-8):1183–95.
9 <https://doi.org/10.1016/j.compositesb.2008.03.010>.
- 10 [31] Boonstra M, van Hest F. The findings of the first survey into plastic bottle cap pollution on beaches
11 in the Netherlands. [07th June 2019]; Available from:
12 http://www.noordzee.nl/project/userfiles//SDN_Doppenrapport_EN_2017_DEF_small.pdf.
- 13 [32] Aver K. 360: Bottle Caps. [07th June 2019]; Available from: [http://www.earth911.com/food/360-](http://www.earth911.com/food/360-bottle-caps)
14 [bottle-caps](http://www.earth911.com/food/360-bottle-caps).
- 15 [33] Oliveira PR, Bonaccorsi AMS, Panzera TH, Christoforo AL, Scarpa F. Sustainable sandwich
16 composite structures made from aluminium sheets and disposed bottle caps. *Thin-Walled Structures*
17 2017;120:38–45. <https://doi.org/10.1016/j.tws.2017.08.013>.
- 18 [34] Oliveira PR, Panzera TH, Freire RT, Scarpa F. Sustainable sandwich structures made from bottle
19 caps core and aluminium skins: A statistical approach. *Thin-Walled Structures* 2018;130:362–71.
20 <https://doi.org/10.1016/j.tws.2018.06.003>.
- 21 [35] Oliveira PR, Kilchert S, May M, Panzera TH, Scarpa F, Hiermaier S. Eco-friendly sandwich panel
22 based on bottle caps core and sustainable components: Static and dynamic characterisation. *Composites*
23 *Part C: Open Access* 2020;3:100069. <https://doi.org/10.1016/j.jcomc.2020.100069>.
- 24 [36] Hu LL, He XL, Wu GP, Yu TX. Dynamic crushing of the circular-celled honeycombs under out-
25 of-plane impact. *International Journal of Impact Engineering* 2015;75:150–61.
26 <https://doi.org/10.1016/j.ijimpeng.2014.08.008>.
- 27 [37] Oliveira PR, dos Santos JC, Ribeiro Filho SLM, Torres Ferreira B, Panzera TH, Scarpa F. Eco-
28 friendly Sandwich Panel Based on Recycled Bottle Caps Core and Natural Fibre Composite Facings.
29 *Fibers Polym* 2020;21(8):1798–807. <https://doi.org/10.1007/s12221-020-9818-7>.
- 30 [38] Hallak Panzera T, Jeannin T, Gabrion X, Placet V, Remillat C, Farrow I et al. Static, fatigue and
31 impact behaviour of an autoclaved flax fibre reinforced composite for aerospace engineering.
32 *Composites Part B: Engineering* 2020;197:108049. <https://doi.org/10.1016/j.compositesb.2020.108049>.
- 33 [39] Montgomery DC. *Design and analysis of experiments*. 7th ed. Hoboken, NJ: Wiley; 2009.

- 1 [40] ASTM International. ASTM C393 - Standard Test Method for Core Shear Properties of Sandwich
2 Constructions by Beam Flexure. West Conshohocken, PA. https://doi.org/10.1520/C0393_C0393M-11.
- 3 [41] ASTM International. ASTM D790 - Standard Test Methods for Flexural Properties of
4 Unreinforced and Reinforced Plastics and Electrical Insulating Materials. West Conshohocken, PA.
5 <https://doi.org/10.1520/D0790-17>.
- 6 [42] ASTM International. ASTM D7250 - Standard Practice for Determining Sandwich Beam Flexural
7 and Shear Stiffness. West Conshohocken, PA. https://doi.org/10.1520/D7250_D7250M-16.
- 8 [43] ASTM International. ASTM C20 - Standard Test Methods for Apparent Porosity, Water
9 Absorption, Apparent Specific Gravity, and Bulk Density of Burned Refractory Brick and Shapes by
10 Boiling Water. West Conshohocken, PA. <https://doi.org/10.1520/C0020-00R10>.
- 11 [44] ASTM International. ASTM D7136 - Standard Test Method for Measuring the Damage Resistance
12 of a Fiber-Reinforced Polymer Matrix Composite to a Drop-Weight Impact Event. West Conshohocken,
13 PA. https://doi.org/10.1520/D7136_D7136M-15.